Yuan Zhanwei*, Li Fuguo and Ji Guoliang

A Modified Johnson Cook Constitutive Model for Aermet 100 at Elevated Temperatures

DOI 10.1515/htmp-2016-0096
Received May 21, 2016; accepted December 30, 2016

Abstract: The predicted flow behaviors of Aermet 100 steel were analyzed within a wide range of temperatures of 1,073 K–1,473 K and strain rates of 0.01 s^{-1}–50 s^{-1} based on isothermal compression tests. Using the original Johnson Cook (JC) model and a modified Johnson Cook (MJC) model, the constitutive equations were constructed in the case of elevated temperatures. For both the JC and MJC, and the previously studied (Arrhenius-type model and double-multivariate nonlinear regression (DMNR)) models, their respective predictability levels were evaluated by contrasting both the correlation coefficient R and the average absolute relative error ($AARE$). The results showed that the prediction from the three models meet the accuracy requirement based on the experimental data, the only exception being the JC model. By comparing the predictability and numbers of material constants involved, the modified Johnson Cook model is regarded as an excellent choice for predicting the flow behaviors of Aermet 100 steel within the range being studied.

Keywords: Aermet 100, constitutive model, modified Johnson Cook model

Introduction

Aermet 100 is a Co-Ni secondary hardening type ultrahigh strength steel that is highly resistant against stress corrosion cracking and fatigue. Common for a typical metal, it possesses excellent strength and ductility. Aermet 100 steel is widely used in aeronautical and astronautical applications [1–4]. The flow behavior of the alloy is an important property vis-à-vis processing and applications due to the complex combination of strain, strain rates, and temperatures [3–8]. A constitutive equation can represent the material's flow behavior and has been widely used as inputs for finite element analyses to simulate the response of materials under specific processing conditions [9]. This alloy has been scarcely studied, and is relatively absent from literature [1–3, 10, 11]. Ji et al. [11] comparatively studied the predictability of the Arrhenius-type constitutive model and artificial neural network (ANN) model of the Aermet 100 steel. Yuan et al. [3] constructed a constitutive model of Aermet 100 steel using a double-multivariate nonlinear regression (DMNR). Also, by using a Split-Hopkinson pressure bar, Hu et al. [1] established a simplified Johnson-Cook model to describe the strain-rate dependent behaviors of Aermet 100 steel.

Several empirical, semi-empirical, phenomenological, and physically-based constitutive models have been proposed for the past few decades [12–17]. The JC model has been widely used as it requires lesser number of experimental data to determine material constants within a wide range of temperatures and strain rates [16, 18–20]. However, the JC model is sometimes incapable of tracking experimental values due to the fact that this model does not take into account the coupled effects of temperatures, strain rates, and temperature upon flow behaviors [18, 21]. In order to address this shortcoming, a modification to the JC model has been proposed and implemented, which was subsequently successful in predicting high temperature flow behavior [19, 20, 22, 23]. Moreover, the sine-hyperbolic law in the Arrhenius type equation has been successfully used, at high accuracy levels, to predict the high temperature flow behavior of materials [6, 11, 16, 19, 20]. However, this type of model contains more material constants compared to its empirical counterparts [17]. A double multiple nonlinear regression (DMNR) model has been proposed by the authors, which considers the entire coupled effect of deformation parameters, strain, strain rates and temperatures that are applicable to Aermet 100 at high accuracy levels [3, 15].

The strain compensation Arrhenius-type model and DMNR of Aermet 100 steel have been previously established [3, 11]. Generally, an ideal constitutive equation should involve a reasonable number of material constants that can be calculated from limited experimental data while being able to represent the flow behavior of the

***Corresponding author: Yuan Zhanwei,** School of Material Science & Engineering, Chang'an University, Xi'an, Shaanxi 710061, China, E-mail: yuanyekingfly@163.com
Li Fuguo, State Key Laboratory of Solidification Processing, School of Materials Science and Engineering, Northwestern Polytechnical University, Xi'an 710072, China
Ji Guoliang, School of Materials Science and Engineering, Henan Polytechnic University, Jiaozuo 454000, China

material at acceptable levels of accuracy and reliability over a wide processing range. However, for both the established constitutive models, there are way too many material constants, making it inconvenient for representing the flow behavior of this alloy. Therefore, a convenient constitutive model needs to be evaluated and validated. The original and modified Johnson Cook constitutive model can be used for this purpose, due to the fact they work with relatively fewer materials constants. After constructing the original and modified Johnson Cook constitutive equation, the accuracy, the number of material constants involved, and the influence of deformation parameters of the constitutive equation are evaluated by comparing it to the Arrhenius-type and DMNR models.

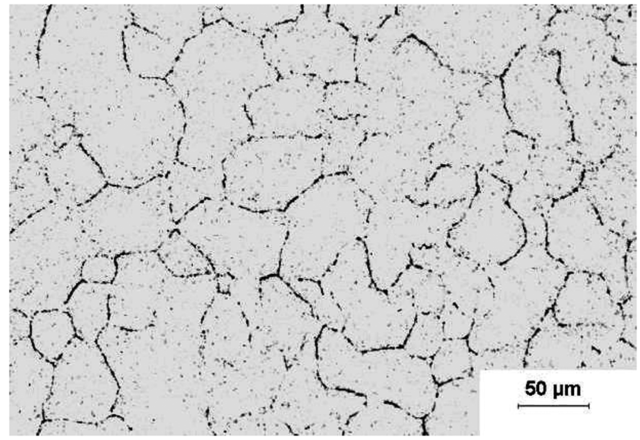

Figure 1: Microstructure of microstructure of as received Aermet 100 steel.

Experimental procedure

The chemical composition of Aermet 100 steel used in this work is tabulated in Table 1. Its initial microstructure is shown in Figure 1. A Gleeble-3800 thermo-mechanical simulator system was used to conduct the isothermal constant strain rate compression test. Cylindrical specimens (8 mm in diameter and 12 mm in height) for the compression tests were machined to produce flat bottomed grooves on the end faces so that it can retain the graphite lubricant that will reduce the interfacial friction between the tools and metals. The compression tests were carried out within a temperature range of 1,073–1,473 K (1,073 K, 1,173 K, 1,273 K, 1,373 K, 1,423 K and 1,473 K), strain rate range of 0.01–50 s^{-1} (0.01 s^{-1}, 0.1 s^{-1}, 1 s^{-1}, 10 s^{-1} and 50 s^{-1}), and a true strain of 0.9. The stress–strain data at multiple temperatures and strain rates were automatically recorded.

Table 1: Chemical composition of Aermet 100 steel (in wt.%).

C	Ni	Co	Cr	Mo	Fe
0.23	11.73	13.85	3.13	1.25	Bal.

Results

Johnson Cook (JC) model

According to the JC model, the flow stress is expressed as [12, 18]:

$$\sigma = (A + B\varepsilon^n)(1 + C\ln\dot{\varepsilon}^*)(1 - T^{*m}) \tag{1}$$

where σ is flow stress, A is the yield stress at reference temperature and strain rate, B is the coefficient of strain hardening, n is the exponent of strain hardening, ε is the true strain, $\dot{\varepsilon}^* = \dot{\varepsilon}/\dot{\varepsilon}_{ref}$ is the dimensionless strain rate with $\dot{\varepsilon}$ being the strain rate (s^{-1}), $\dot{\varepsilon}_{ref}$ the reference strain rat (s^{-1}), and T^* is homologous temperature, expressed as:

$$T^* = \frac{T - T_{ref}}{T_m - T_{ref}} \tag{2}$$

where T_m is the melting temperature of the material, T is deformation temperature, and T_{ref} is the reference temperature ($T \geq T_{ref}$). C and m are material constants that represent the coefficient of strain rate hardening and thermal softening exponent, respectively. Accordingly, the three items in the expression from the left to right represents the strain hardening effect, strain rate strengthening effect, and temperature effect, with the total effect obtained by multiplying the aforementioned terms. The procedure for determining the material constant is presented in Figure 2. In this experiment, the reference temperature is T_{ref} = 1,073 K, and the reference strain rate was $\dot{\varepsilon}_{ref} = 0.01$ s^{-1}. Under the reference deformation conditions, the yield stress is A = 166.1 MPa. The melting point T_m of Aermet 100 steel is 1,803 K. After regression, the material constants of the JC model for Aermet 100 steel are given in Table 2.

Then, the Johnson Cook constitutive equation for Aermet 100 steel is:

$$\sigma = (166.1 + 34.3\varepsilon^{0.9679})(1 + 0.0839\ln\dot{\varepsilon}^*)(1 - T^{*0.5718}) \tag{3}$$

From eq. (3), it can be seen that the exponent of strain hardening n is 0.9679, which exceeds the normal range

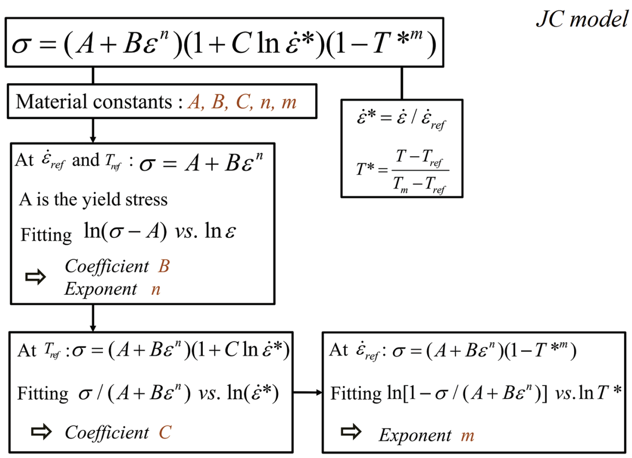

Figure 2: The procedure of JC model.

Table 2: Parameters for the JC model.

Parameter	*A*	*B*	*C*	*n*	m
Value	166.1	34.3	0.0839	0.9679	0.5718

(0–0.5). According to the established constitutive equation, the experimental and predicted flow stress for Aermet 100 at various processing conditions is shown in Figure 3. Comparing the experimental and predicted results, it can be seen that the predicted flow stresses exhibit a significant deviation in most loading conditions, especially at low strain rates. In certain deformation conditions, the predicted flow stress data is capable of tracking the experimental data, such as middle strain rates. This may be due to the influencing factors of strain, strain rates, and temperatures being mutually independent in the JC model, without taking into account the accumulation effect of any other influencing factor [19].

Modified Johnson Cook（MJC）model

The values obtained from the JC model for the predicted flow stress do not agree with the experimental data. Therefore, a modified Johnson Cook model was used instead, which is [19]:

$$\sigma = (A_1 + B_1\varepsilon + B_2\varepsilon^2)(1 + C_1 \ln \dot{\varepsilon}^\star)\exp[(\lambda_1 + \lambda_2 \ln \dot{\varepsilon}^\star)T^\star] \tag{4}$$

where σ is flow stress, ε is the true strain, $\dot{\varepsilon}^\star = \dot{\varepsilon}/\dot{\varepsilon}_0$ is the dimensionless strain rate with $\dot{\varepsilon}$ being the strain rate, and $\dot{\varepsilon}_0$ the reference strain rate $T^\star = T - T_{ref}$, with T and T_{ref} being the current and reference temperatures, respectively, while A_1, B_1, B_2, C_1, λ_1 and λ_2 are the materials constants. The reference temperature and strain rates are set to 1,073 K and 0.01 s^{-1}, respectively.

When the deformation temperature is 1,073 K and the strain rate is 0.01 s^{-1}, eq. (4) can be expressed as follows:

$$\sigma = A_1 + B_1\varepsilon + B_2\varepsilon^2 \tag{5}$$

After fitting the stress–strain data, the values of A_1, B_1 and B_2 were determined to be 172.16 MPa, 69.08 MPa, and −72.84 MPa, respectively. The fitting results are shown in Figure 4.

When the deformation temperature is the reference temperature, eq. (4) becomes:

$$\frac{\sigma}{A_1 + B_1\varepsilon + B_2\varepsilon^2} = 1 + C_1 \ln \dot{\varepsilon}^\star \tag{6}$$

Substituting five different strain rates and corresponding flow stress at different strains into eq. (6), the values of C_1 can be obtained from the slope of the lines in the $\sigma/(A_1 + B_1\varepsilon + B_2\varepsilon^2) - \ln(\dot{\varepsilon}^\star)$ plot. Figure 5 illustrates the variation of $\sigma/(A_1 + B_1\varepsilon + B_2\varepsilon^2)$ with $\ln(\dot{\varepsilon}^\star)$ at the temperature of 1,073 K, and it can be seen that the slope consequently varies within a very small range. Then, the material constant C_1 can be determined using the linear fitting method, which results in a value of 0.08324.

Then, a new parameter $\lambda = \lambda_1 + \lambda_2 \ln \dot{\varepsilon}^\star$ was introduced, which is only a function of the strain rate, allowing us to change eq. (4) into:

$$\frac{\sigma}{(A_1 + B_1\varepsilon + B_2\varepsilon^2)(1 + C_1 \ln \dot{\varepsilon}^\star)} = e^{\lambda T^\star} \tag{7}$$

Taking the logarithm of both sides of eq. (7), it becomes eq. (8):

$$\ln\left[\frac{\sigma}{(A_1 + B_1\varepsilon + B_2\varepsilon^2)(1 + C_1 \ln \dot{\varepsilon}^\star)}\right] = \lambda T^\star \tag{8}$$

For different strain rates and deformation temperatures, the relationship between $\ln[\frac{\sigma}{(A_1 + B_1\varepsilon + B_2\varepsilon^2)(1 + C_1 \ln \dot{\varepsilon}^\star)}]$ and $T^\star$ is viable and can be determined. The mean values of $\ln[\frac{\sigma}{(A_1 + B_1\varepsilon + B_2\varepsilon^2)(1 + C_1 \ln \dot{\varepsilon}^\star)}]$ at fifteen strain values are used to determine the values of λ. The values of λ for five different strain rates can be obtained from the slopes of the linear fitting plots. The values of λ_1 and λ_2 can be obtained from the intercept and slope of line$\lambda - \ln \dot{\varepsilon}^\star$, respectively, where $\lambda_1 = -0.00533$ and $\lambda_2 = 0.0003044$ (Figure 6). The procedure for evaluating material constants using the modified Johnson Cook model is shown in Figure 7.

The parameters of the modified Johnson Cook model for Aermet 100 are tabulated in Table 3.

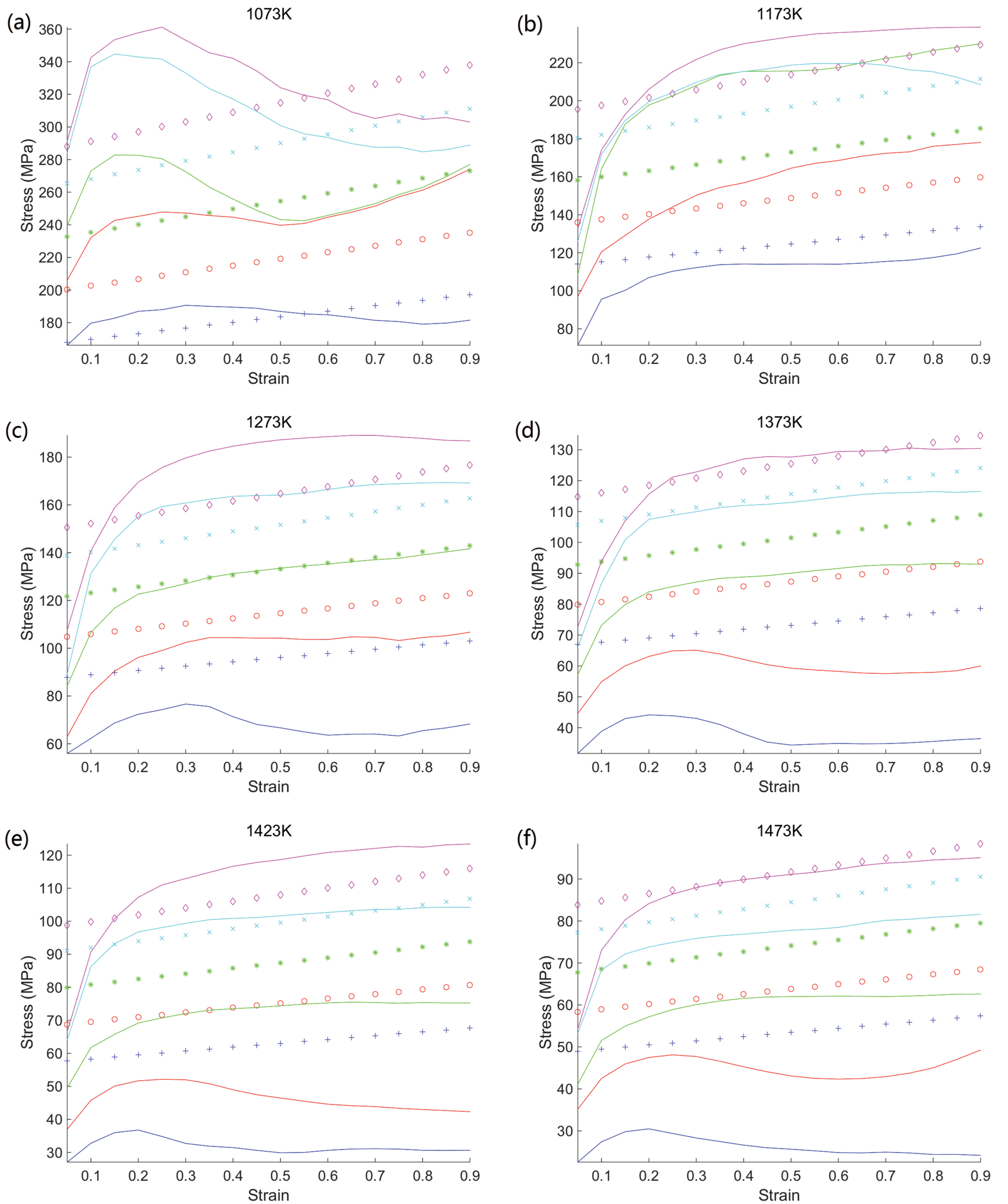

Figure 3: Comparison between the experimental and predicted flow stress from JC model at deformation temperature (a) 1,073 K, (b) 1,173 K, (c) 1,273 K, (d) 1,373 K, (e) 1,423 K, and (f) 1,473 K (colors represent: blue 0.01 s^{-1}, red 0.1 s^{-1}, green 1 s^{-1}, cyan 10 s^{-1}, magenta 50 s^{-1}. Lines draw the experimental data and symbols represent predicted results).

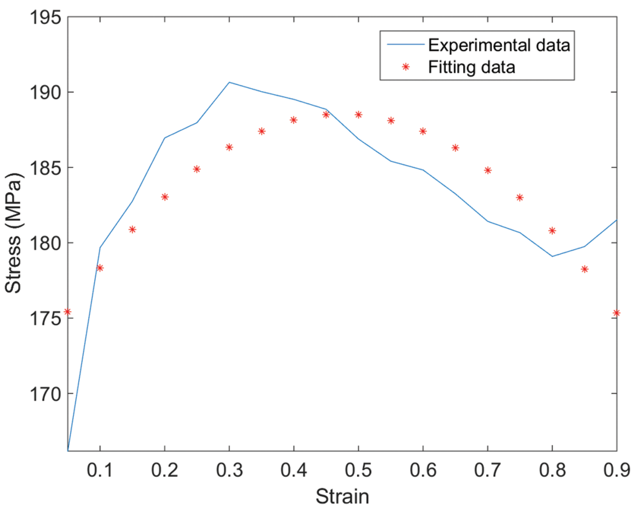

Figure 4: Relationship between σ and ε at the temperature of 1,073 K, strain rate 0.01 s^{-1}.

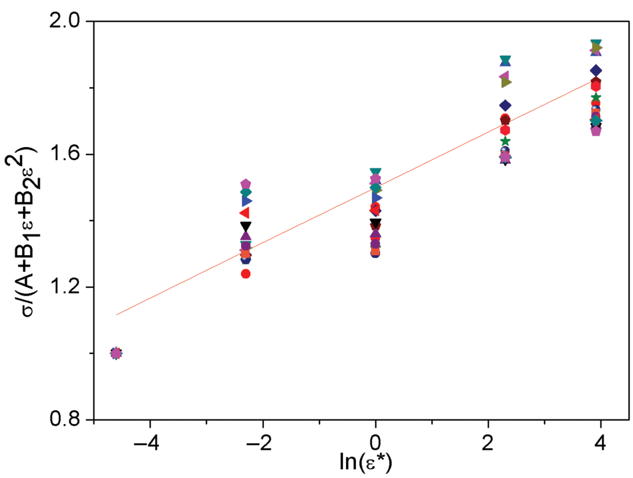

Figure 5: Relationship between $\sigma/(A_1 + B_1\varepsilon + B_2\varepsilon^2)$ and $\ln(\dot{\varepsilon}^*)$ at the temperature of 1,073 K (the symbol represent different strain).

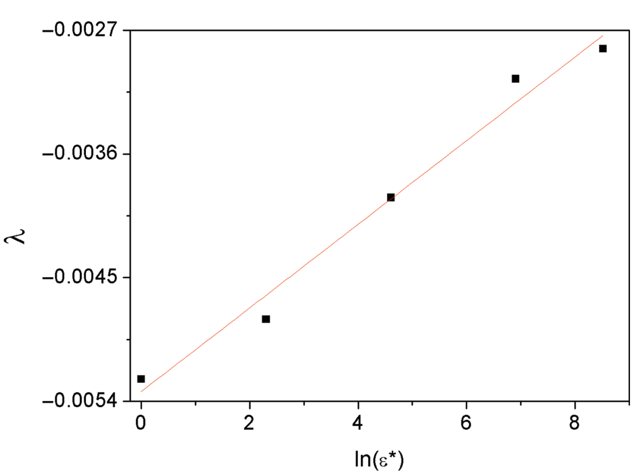

Figure 6: Relationship between $\lambda$and $\ln\dot{\varepsilon}^*$.

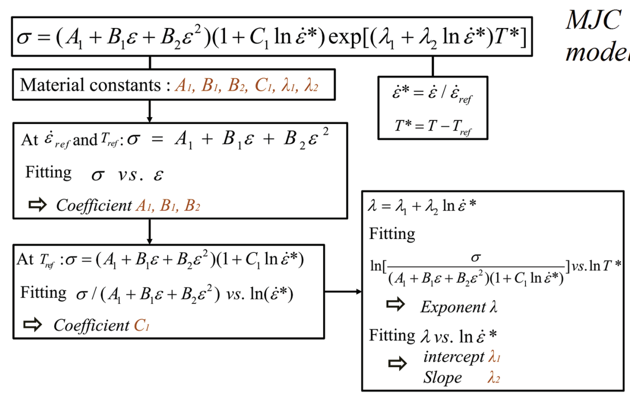

Figure 7: The procedure of modified Johnson Cook model.

Table 3: Parameters for the modified Johnson Cook model.

Parameter	A_1	B_1	B_2	C_1	λ_1	λ_2
Value	172.16	69.08	−72.84	0.08324	−0.00533	0.0003044

The relationship between stress σ, strain ε, deformation rate $\dot{\varepsilon}$, and deformation temperature T is established based on the modified Johnson Cook model:

$$\sigma = (172.16 + 69.08\varepsilon - 72.84\varepsilon^2)(1 + 0.08324 \ln \dot{\varepsilon}^*) \times \exp[(-0.00533 + 0.0003044 \ln \dot{\varepsilon}^*)T^*] \quad (9)$$

The predicted flow stress according to the modified Johnson Cook constitutive equation is shown in Figure 8. It can be seen that the predicted flow stress value from the constitutive equation could track the experimental data pertaining to Aermet 100 steel under most deformation conditions.

Discussion

In order to analyze the accuracy of the constitutive equation, the comparison of stress values between experimental and predicated values for the JC, MJC, strain compensation Arrhenius-type model [11], and DMNR [3] is shown in Figure 9. It is obvious that the predictions agree with the experimental results in the case of these methods. However, it can also be seen that they are unable to accurately predict high stresses, especially at low temperatures and strain rates greater than 1 s^{-1}. The original JC model is unable to adequately represent the high temperature flow behavior of Aermet 100 steel, as they lack the couple effect that is inherent in the deformation parameters. For the MJC, Arrhenius-type, and

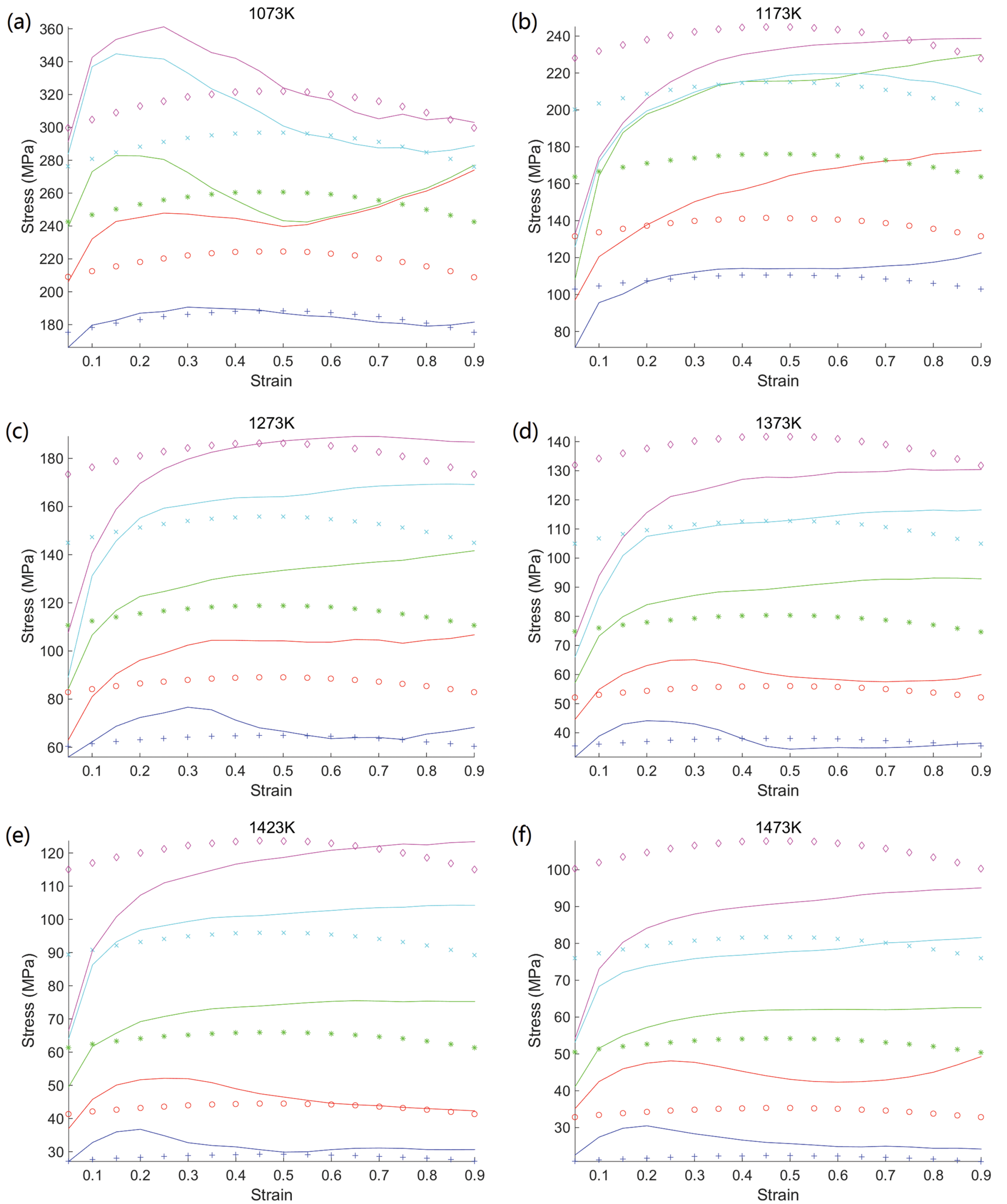

Figure 8: Comparison between the experimental and predicted flow stress from MJC model at deformation temperature (a) 1,073 K, (b) 1,173 K, (c) 1,273 K, (d) 1,373 K, (e) 1,423 K, and (f) 1,473 K (colors represent: blue 0.01 s^{-1}, red 0.1 s^{-1}, green 1 s^{-1}, cyan 10 s^{-1}, magenta 50 s^{-1}. Lines draw the experimental data and symbols represent predicted results).

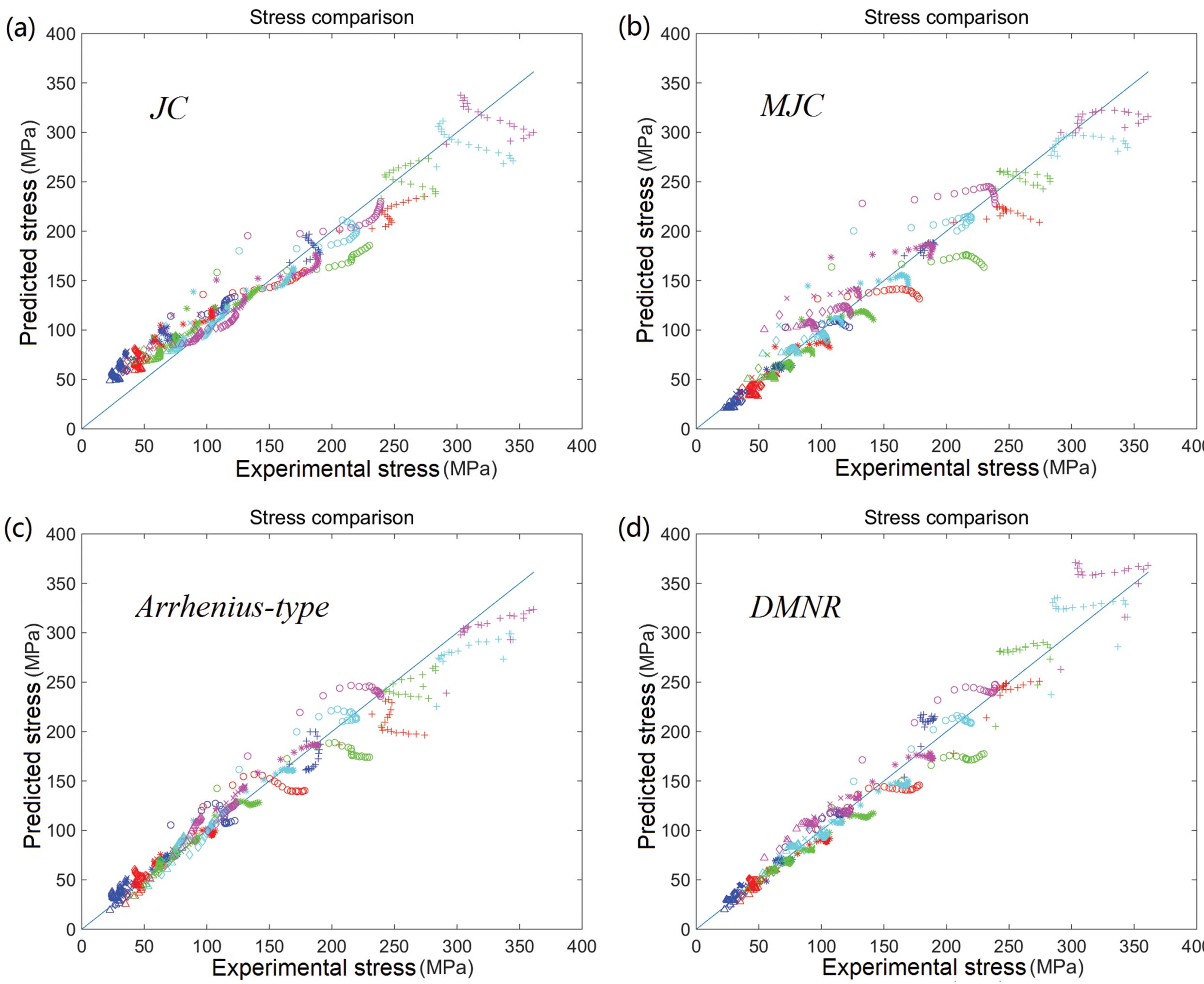

Figure 9: The comparison between the experiment results and predicted results by (a) JC model; (b) MJC model; (c) Arrhenius-type; (d) DMNR (symbols represent: "+" 1,073 K, "o" 1,173 K, "*" 1,273 K, "×" 1,373 K, "◊" 1,423 K, "Δ" 1,473 K) (colors represent: blue 0.01 s^{-1}, red 0.1 s^{-1}, green 1 s^{-1}, cyan 10 s^{-1}, magenta 50 s^{-1}).

DMNR models, the predicted stress (low) agrees with the experimental results.

The predictability of the developed constitutive equation is quantified in terms of the correlation coefficient (R) and average absolute relative error ($AARE$), and expressed as [3, 11]:

$$R = \frac{\sum_{i=1}^{N}(E_i - \bar{E})(P_i - \bar{P})}{\sqrt{\sum_{i=1}^{N}(E_i - \bar{E})^2 \sum_{i=1}^{N}(P_i - \bar{P})^2}} \tag{10}$$

$$AARE(\%) = \frac{1}{N}\sum_{i=1}^{N}\left|\frac{E_i - P_i}{E_i}\right| \times 100 \tag{11}$$

where E is the experimental flow stress (MPa) and P is the predicted flow stress (MPa), obtained from the developed constitutive equation. $\bar{E}$ and $\bar{P}$are the mean values of E and P, respectively. N is the total number of data used in this study.

Figure 10 show the predictability of the four methods. The values of R of the four methods (JC, MJC, Arrhenius-type, and DMNR) are 0.9733, 0.9749, 0.9861, and 0.9805, while the $AARE$ are 25.05 %, 10.92 %, 7.62 % and 9.22 %, respectively. The results of R and $AARE$ reflect the excellent prediction capabilities of the developed constitutive equations for the last three models, with the exception of the JC model. The values of R and $AARE$ of the modified Johnson Cook constitutive equation is relatively not very accurate compared to that of the Arrhenius-type and DMNR models. However, it can also be seen that the number of material constants involved in the modified Johnson Cook constitutive equation is only 6, while 32 material constants are involved in the strain compensation of the Arrhenius-type model [11], and 12 material

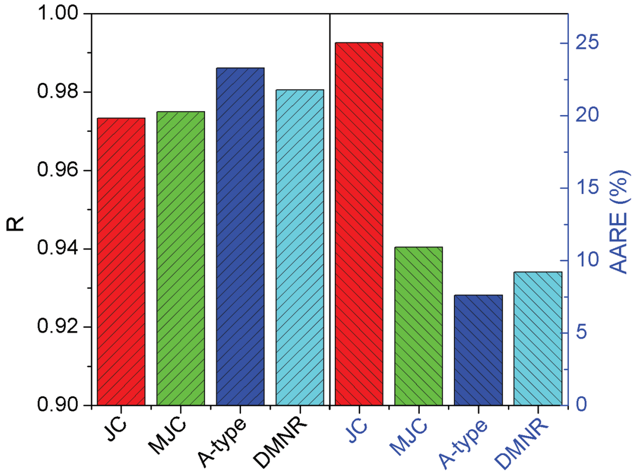

Figure 10: The predictability of these four models.

constants are involved in the DMNR model [3]. This proves that the modified Johnson Cook constitutive equation can produce reasonable values more efficiently using fewer material constants to describe the high temperature flow behavior of Aermet 100 steel.

Additionally, Figures 11 and 12 show the plots of influences of deformation parameters on the predictability of these models within selected ranges (temperatures, strain rates, and strains) according to eqs (14) and (15). It can be seen that temperature has a great influence on the predictability of these four models, especially for the JC and MJC models. For the JC model, the term homologous temperature is introduced; however, it lacks enough couple effect vis-à-vis temperature-strain and temperature-strain rates [21]. For the other models, the couple effect with temperature proved sufficient. Strain affects the predictability of these models. However, the predicted results show increased variation at lower strain values. Strain rates significantly influence predictability. For the JC model, at low strain rates, the predictability is poor, while at higher strain rates, the predictability is better. A similar trend is evident for the Arrhenius-type model. The accuracy can be improved by modifying the JC model by accounting for the effect of strain rates and temperatures. In the context of predictability and convenience, the modified Johnson Cook model is an excellent choice.

Conclusions

The flow behavior of Aermet 100 has been studied based on hot compression tests performed in the temperature range of 1,073–1,473 K (1,073 K–1,473 K) and strain rates of 0.01–50 s^{-1}. Previous studies on constitutive model of Aermet 100 (Arrhenius-type model and DMNR) reported excellent predictability. However, there were too many material constants, which is inconvenient in the context of finite element applications. It can be concluded that:

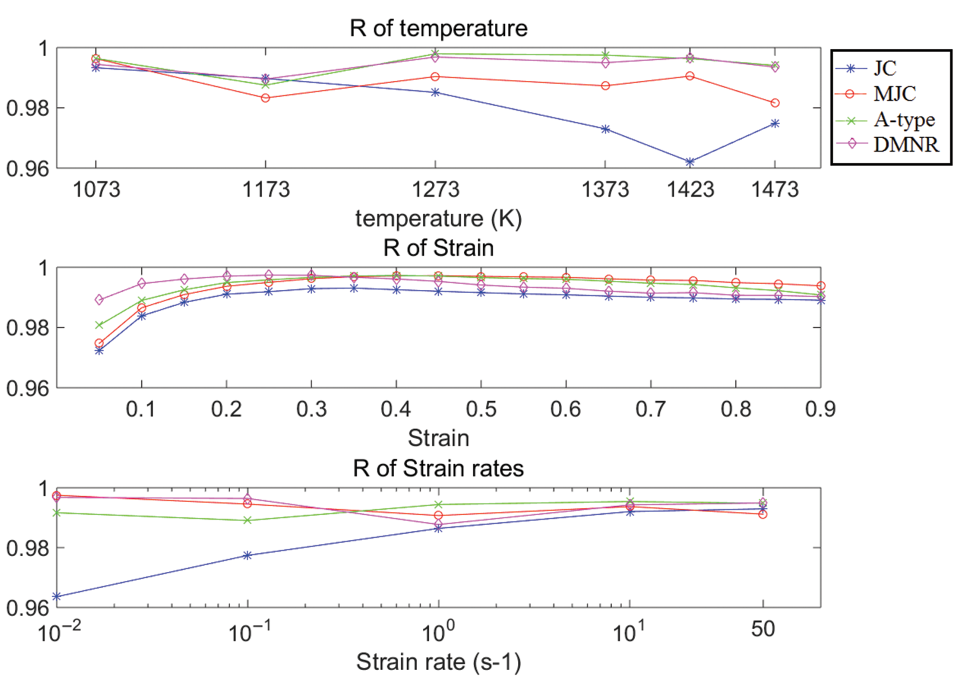

Figure 11: The correlation coefficient *R* distribution for three deformation parameters of these four models.

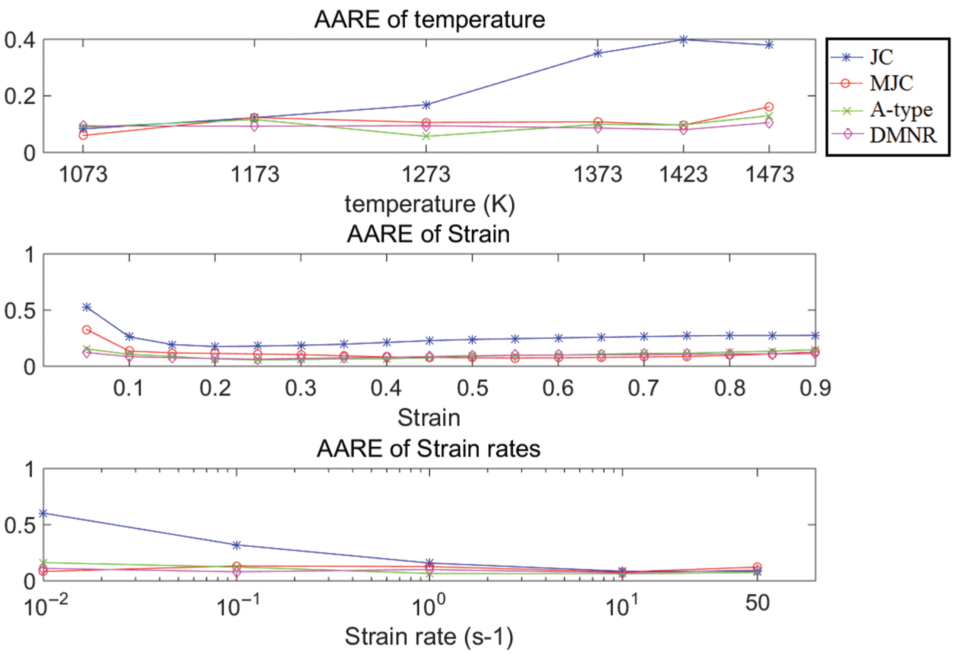

Figure 12: The *AARE* distribution for three deformation parameters of these four models.

(1) Both the original Johnson Cook and modified Johnson Cook models were introduced to predict flow behavior of Aermet 100 at elevated temperatures. The predicted results show that the modified Johnson Cook constitutive model can inadequately and precisely predict flow stress under most deformation conditions.

(2) The predictability of the constitutive models, including the JC, MJC, strain compensation Arrhenius-type model, and DMNR were evaluated in the context of correlation coefficient (R) and average absolute relative error (*AARE*). It was confirmed that the predictability of Arrhenius-type and DMNR modified models are relatively more accurate than the Johnson Cook constitutive equation, while the modified Johnson Cook constitutive equation require relatively fewer material constants. All in all, the modified Johnson Cook model is an excellent choice for predictability and convenience.

Funding: The authors are very grateful for the support received from National Natural Science Foundation of China (No. 51504037 and 51605387), National key research and development program (No. 2016YFB1100103), Natural Science Foundation of Shaanxi Province (No. 2014JQ6210), the Special Fund for Basic Scientific Research of Central Colleges, Chang'an University (2014G1311090 and 310831161023) and Special Fund for Innovation Team Research of Central Colleges (310831163401). And Supported by the fund of the State Key Laboratory of Solidification Processing in NWPU (No. SKLSP201646).

References

[1] D.Y. Hu, K.P. Meng, H.L. Jiang, J. Xu and R.R. Liu, Mater. Design., 87 (2015) 759–772.
[2] D. Hu, K. Meng and H. Jiang, Procedia Eng., 99 (2015) 1459–1464.
[3] Z. Yuan, F. Li, H. Qiao and G. Ji, J. Mater. Eng. Perform., 23 (2014) 1–19.
[4] H. Qiao, F. Li, G. Ji and M. Xiao, Rare Met. Mater. Eng., 43 (2014) 926–931.
[5] Y. Zhang, A.A. Volinsky, Q.Q. Xu, Z. Chai, B. Tian, P. Liu and T.T. Hai, Metall. Mater. Trans. A, 46 (2015) 5871–5876.
[6] S.M. Abbasi, M. Morakkabati, A.H. Sheikhali and A. Momeni, Metall. Mater. Trans. A, 45 (2014) 5201–5211.
[7] G. Quan, J. Liu, A. Mao, B. Liu and J. Zhang, High Temp. Mater. Proc., 34 (2015) 643–650.
[8] Y. Chen, C. Luo, J. Wang, Y. Zhao and H. Chen, High Temp. Mater. Proc., 35 (2016) 29–35.
[9] K.P. Rao, Y.V.R.K. Prasad and K. Suresh, Mater. Design., 32 (2011) 2545–2553.
[10] D. Figueroa and M.J. Robinson, Corros. Sci., 52 (2010) 1593–1602.
[11] G. Ji, F. Li, Q. Li, H. Li and Z. Li, Mat. Sci. Eng. A, 528 (2011) 4774–4782.

[12] G.R. Johnson and W.H. Cook, Proceedings of the 7th International Symposium on Ballistics, The Netherlands, 1983, 541–547.
[13] F.J. Zerilli and R.W. Armstrong, J. Appl. Phys., 61 (1987) 1816–1825.
[14] J. Li, F. Li, J. Cai, R. Wang, Z. Yuan and G. Ji, Comp. Mater. Sci., 71 (2013) 56–65.
[15] Z. Yuan, F. Li, H. Qiao, M. Xiao, J. Cai and J. Li, Mat. Sci. Eng. A, 578 (2013) 260–270.
[16] J. Cai, K. Wang and Y. Han, High Temp. Mater. Proc., 35 (2015) 297–307.
[17] Z. Yuan, F. Li, G. Ji, H. Qiao and J. Li, J. Mater. Eng. Perform., 23 (2014) 1016–1027.
[18] A. Abbasi-Bani, A. Zarei-Hanzaki, M.H. Pishbin and N. Haghdadi, Mech. Mater., 71 (2014) 52–61.
[19] A. He, X. Wang, G. Xie and H. Zhang, Mater. Design., 52 (2013) 677–685.
[20] D. Samantaray, S. Mandal and A.K. Bhaduri, Comp. Mater. Sci., 47 (2009) 568–576.
[21] Y.C. Lin and X.M. Chen, Mater. Design., 32 (2011) 1733–1759.
[22] W. Song, J. Ning, X. Mao and H. Tang, Mat. Sci. Eng. A, 576 (2013) 280–289.
[23] Y.P. Wang, C. Han, C. Wang and S. Li, J. Mater. Sci., 46 (2011) 2922–2927.